

PAPER • OPEN ACCESS

## Influences of Cooling Rate and Dendrite Morphology Assumptions on the Cracking Susceptibility of Ternary Al-Cu-Si Alloys during Solidification

To cite this article: Guangwei Zhao *et al* 2019 *IOP Conf. Ser.: Mater. Sci. Eng.* **562** 012047

View the [article online](#) for updates and enhancements.



**IOP | ebooks™**

Bringing you innovative digital publishing with leading voices to create your essential collection of books in STEM research.

Start exploring the collection - download the first chapter of every title for free.

# Influences of Cooling Rate and Dendrite Morphology Assumptions on the Cracking Susceptibility of Ternary Al-Cu-Si Alloys during Solidification

Guangwei Zhao<sup>1,2</sup>, Chong Ding<sup>2</sup> and ChenJian<sup>2</sup>

1 Hubei Key Laboratory of Hydroelectric Machinery Design & Maintenance, China Three Gorges University, Yichang 443002, China

2 College of Mechanical and Power Engineering, China Three Gorges University, Yichang 443002, China

Email: zgwhit@163.com

**Abstract.** The hot cracking susceptibility of ternary Al-Cu-Si alloys in Al rich corner were calculated using the author's own program which was coupled with a CALPHAD software Thermo-Calc for phase diagram information. The influences of cooling rate and dendrite morphology assumptions on the hot cracking susceptibility of Al-Cu-Si alloys were mainly considered. It is found that the hot crack susceptibility of high cooling rate is more serious than that of low cooling rate and the alloys tending to form more eutectic phases have higher thermal cracking sensitivity. In addition, the predicted results show that the calculated susceptibility under the assumption of dendrite morphologies extraction in the middle or end stage of solidification, such as inward cylindrical, inward spherical and plate dendrite, are relatively higher than that of the initial stage of solidification, such as spherical and cylindrical dendrite.

## 1. Introduction

Hot crack is a kind of solidification defect often appearing in casting and welding process, which can seriously affect the integrity and service performance of metal parts. Therefore, hot cracking has always been the focus of attention in alloy casting process. Hot cracking usually occurs at the end of solidification and near the temperature of solidus. This is because stress produced by the solidification shrinkage of the casting at the end of solidification exceeds the maximum stress that the alloy can bear. There are many theories of hot cracking mechanism, such as strength theory [1], liquid film theory [2], stress and bridging theory [3], solidification shrinkage compensation theory [4] and so on. There are also many test methods and evaluation criteria for hot cracking sensitivity, such as thermal cracking ring method [5], stress and strain type thermal cracking criterion [6], CSC criterion [3], RDG model [7] and the model of Sindo [8]. In Ref. [8], a very good review of the numerous models for hot tearing in castings and welding can be found.

There are many studies on hot cracking of binary Al-Cu [8] and Al-Si [9] alloys. But at present, Al-Cu-Si ternary alloys are more and more used in industry because of their excellent mechanical and casting properties. There are relatively few studies about the hot cracking properties of ternary Al-Cu-Si alloys. Sindo [8] investigated the hot cracking of ternary Al-Cu-Si, Al-Cu-Mg and Al-Si-Mg alloys, and considered three different conditions of without solid diffusion, with solid diffusion under two cooling rate of 20 and 100 °C/s. However, in the calculation process of Sindo [8], a powerful commercial software Pandat is used, which can not consider the effect of dendrite morphology on the formation of hot cracking. In this paper, the model of Sindo [8] is used to calculate the hot cracking of



ternary Al-Cu-Si alloys by using the author's own program. The effects of solidification rate and dendrite morphology assumption on the hot cracking formation are mainly considered.

## 2. Model Description

In author's previous studies [10, 11], a multiphase solidification model for calculating the solidification paths and micro-segregation of multicomponent alloys was proposed. The model was used to calculate the solidification paths of various ternary Al alloys, such as Al-Cu-Si [10], Al-Si-Mg [11], Al-Zn-Mg [12] and so on. In this model, a unified parameter  $\Phi$  which can consider various factors is proposed. Through setting the relative parameters, the effects of cooling rate, solid diffusion, dendrite morphology and other factors on solidification process can be considered. In this paper, the solidification paths and temperature versus solid fraction curves of Al-Cu-Si alloys in Al-rich corner are calculated based on this model (expressed in the form by Eq. 1~Eq.5). Then, Sindo criterion [8] is calculated by temperature versus solid fraction curves ( $T$ - $f_s$ ) to calculate the hot cracking tendency of the alloy system under different conditions. It should be pointed out that the program in this paper is coupled with Thermo-Calc in order to calculate the thermodynamic data, such as liquidus, solidus, solute partition coefficient and so on.

$$C_{Li}^{\alpha} = C_{0i} [1 - (1 - \Phi_i^{\alpha} k_i^{\alpha}) f_s]^{\frac{k_i^{\alpha} - 1}{1 - \Phi_i^{\alpha} k_i^{\alpha}}} \quad (1)$$

$$C_{Li}^{2E} = C_{0i} [1 - (1 - \Phi_i^{2E} k_i^{2E}) f_s]^{\frac{k_i^{2E} - 1}{1 - \Phi_i^{2E} k_i^{2E}}} \quad (2)$$

$$C_{Li}^{3E} \equiv C_{Li}^{TE} \quad (3)$$

Where,  $C_{Li}^{\alpha}$ ,  $C_{Li}^{2E}$ ,  $C_{Li}^{3E}$ , represent the liquid composition of solute  $i$  in the three solidification stages of an ternary eutectic alloy, i.e., primary solidification, binary eutectic solidification and ternary eutectic solidification, respectively. The unified parameter  $\Phi$  can be expressed as:

$$\Phi_n = \theta_n \cdot \varphi_n / (1 + \theta_n \cdot \varphi_n) \quad (n = 1, 2) \quad (4)$$

Where  $\varphi_n$  is a parameter called fourier diffusion number and can be expressed as:

$$\varphi_n = (D_{ns} / R_f) \zeta \cdot A_{2N} \quad (n = 1, 2) \quad (5)$$

The symbols of  $A_{2N}$  and  $\zeta$  in Eq.(5) represent a basic geometry-unit vector and a normalized weighting vector corresponding to the basic geometry-units  $A_{2N}$ , respectively. Through different designing, the dendrite morphologies of spherical, cylindrical, plate-like, inward cylindrical and inward spherical shapes can be considered by the model [10-13].

In Ref. [8], the author proposed that the maximum steepness  $\left|dT/d(fs)^{1/2}\right|$  can represent the crack susceptibility. In this paper, the solidification path and  $T$ - $f_s$  were from 0 to 5 wt% Cu at the interval of 0.5 wt% Cu and from 0 to 5 wt% Si at the interval of 0.5 wt% Si. Then the maximum steepness  $\left|dT/d(fs)^{1/2}\right|$  of each curve was calculated to construct the cracksusceptibility map for the ternary Al-Cu-Si alloy system using the commercial plotting software Tecplot.

## 3. Calculation Results and Discussion

### 3.1. Influence of Cooling Rate

In this paper, different cooling rates were selected based on the solidification experiment of Al-Cu-Si alloys with three different molds of graphite(5.96°C/s), sand(0.45°C/s) and insulated material (0.068°C/s) [13]. The calculated results for the ternary Al-Cu-Si alloy system with three different

cooling rates are shown in Figure 1. In this group of calculation, the dendrite morphology was assumed to be equiaxed dendrite. In the calculation process, the temperature vs. solid fraction curves ( $T-f_s$ ) were calculated first for the 81 alloys (see the grid intersection in Figure 1) in the Al rich corner. For each alloy, the maximum steepness  $\left|dT/d(f_s)^{1/2}\right|$  (the unit is  $^{\circ}\text{C}$ ) was then plotted against its composition to construct the crack susceptibility map.

It can be seen in Figure 1 the crack susceptibility decreases in the order of graphite mold, sand mold and insulated mold. The crack susceptibilities of the three different situations are  $390.27\sim 1713.34^{\circ}\text{C}$  for insulated mold,  $543.35\sim 1870.48^{\circ}\text{C}$  for sand mold and  $583.19\sim 2378.56^{\circ}\text{C}$  for insulated mold, respectively. In addition, it can be seen in Figure 1 the location of the highest crack susceptibility are slightly different because of different cooling rates. On the one hand, the faster the solidification rate is, the less the solute diffusion is, the higher the solute content in the liquid phase at the end of solidification and the more eutectic phases (as shown in Figure 2 (a)) are, the more serious the tendency of hot cracking is. In addition, the location of the highest hot crack susceptibility is also related to the alloy compositions. The solidification paths of alloys with different compositions are different. In Figure 2(b), it can be seen that the solidification paths of alloys Al-4.0~5.0Cu-1.0Si reached the binary eutectic trough and the ternary eutectic point. Therefore, these alloys tend to form more eutectic phases at the end of solidification, which caused higher cracking sensitivity [5, 8, 9] as shown in Figure 1.

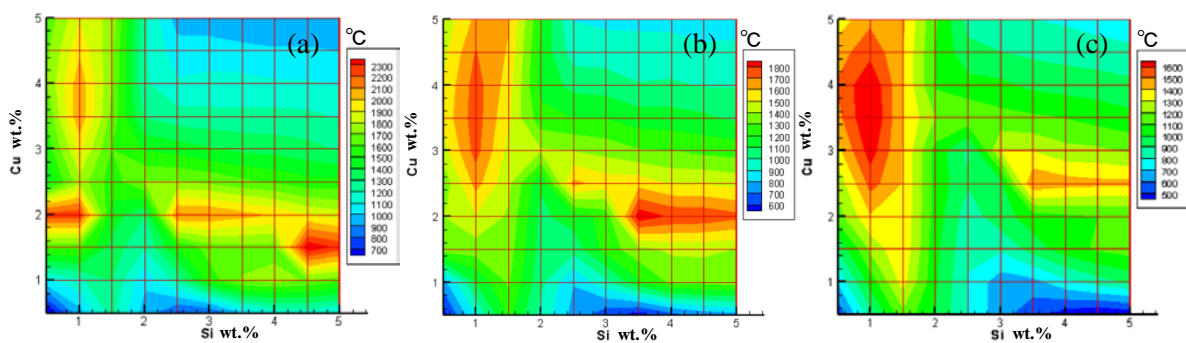


**Figure 1.** Al-Cu-Si hot crack susceptibility maps with different cooling rate: (a) graphite mold ( $5.96^{\circ}\text{C/s}$ ); (b) sand mold ( $0.45^{\circ}\text{C/s}$ ); (c) insulated mold ( $0.068^{\circ}\text{C/s}$ )

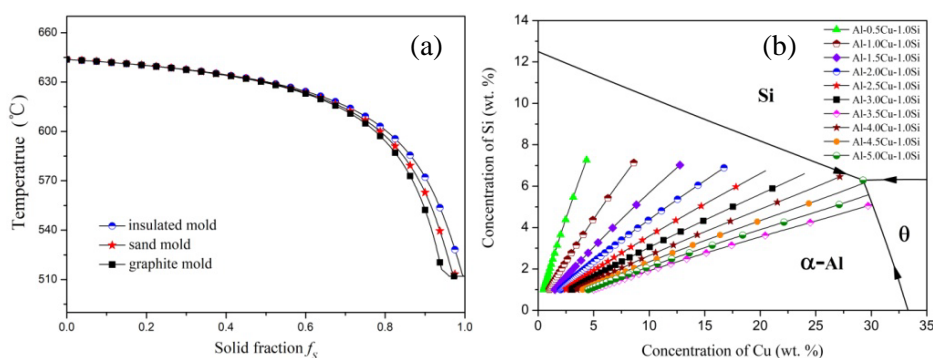


**Figure 2.** Calculated results of the selected alloys: (a)  $T-f_s$  curves of alloy Al-4.0Cu-1.0Si with different cooling rate; (b) solidification paths of Al-0.5~5.0Cu-1.0Si of insulated mold

### 3.2. Influence of Dendrite Morphology

Figure 3 shows the calculated hot crack susceptibility maps with different dendrite morphology assumptions. It can be seen that the assumption of dendrite morphology also can influence the crack susceptibility distribution and the location of the highest position. The crack susceptibility of spherical, cylindrical, plate-like, inward cylindrical, inward spherical, equiaxed dendrite are  $409.95\sim 1714.40^{\circ}\text{C}$ ,  $515.13\sim 1798.46^{\circ}\text{C}$ ,  $586.82\sim 2615.24^{\circ}\text{C}$ ,  $604.72\sim 3142.43^{\circ}\text{C}$ ,  $590.28\sim 3584.43^{\circ}\text{C}$  and

561.58~2165.81°C, respectively. It can be seen that the predicted susceptibility under the assumption of dendrite morphologies extraction in the initial stage of solidification, such as spherical and cylindrical dendrite, are relatively low. The predicted susceptibility under the assumption of dendrite morphologies extraction in the middle or end stage of solidification, such as inward cylindrical, inward spherical and plate dendrite, are relatively high. And all the predicted susceptibility in Figure 3 are between the two extreme situation of lever-rule (344.85~1690.65°C) and that of Scheil model (1066.49~42525.4°C) as shown of Figure 4.

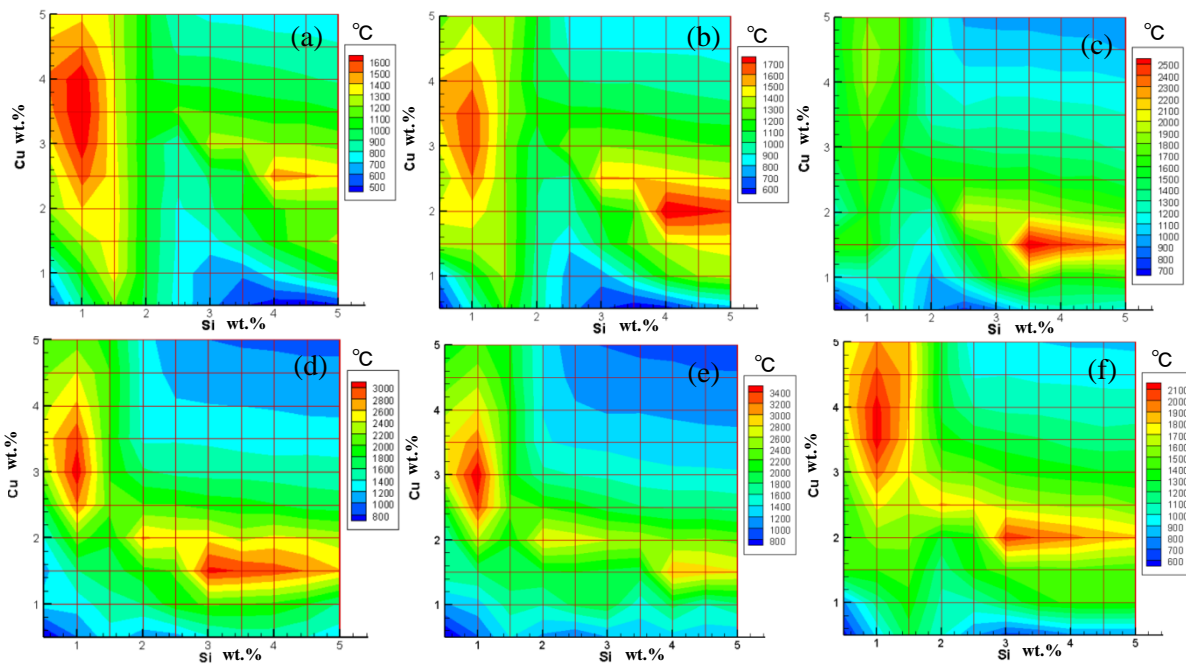


**Figure 3.** Al-Cu-Si hot crack susceptibility maps with different dendrite morphology assumptions: (a) spherical; (b) cylindrical; (c) plate-like; (d) inward cylindrical; (e) inward spherical; (f) equiaxed dendrite

To explain the differences of hot crack susceptibility maps with different dendrite morphology assumptions, a group of solidification paths as shown in Figure 5 were calculated with the same dendrite morphology assumptions for the selected alloys. It can be seen that for the alloy Al-1.0Si-3.5Cu, the dendrite morphology assumptions caused greatly differences in the solidification path of the alloy. The results are distributed between the two limit cases. The results of cylindrical, inward spherical and plate dendrite are closer to Lever-rule, while the results of inward cylindrical, inward spherical and plate dendrite are closer to Scheil model. The results of equiaxed dendrite are in the middle position because the morphology are constructed the other five single morphologies<sup>[14]</sup>.

#### 4. Conclusions

Influences of cooling rate and dendrite morphology assumptions on the susceptibility of ternary Al-Cu-Si alloys to cracking during solidification are investigated. The calculated results indicated that cooling rate and the assumptions dendrite morphology have great influences on hot cracking susceptibility of ternary Al-Cu-Si alloys. The crack susceptibility decreases in the order of graphite mold, sand mold and insulated mold and the value are 390.27~1713.34°C, 543.35~1870.48°C and 583.19~2378.56°C, respectively. It also can be found that the predicted hot crack susceptibility under the assumption of dendrite morphologies extraction from the middle or end stage of solidification, such as inward cylindrical (604.72~3142.43°C), inward spherical (590.28~3584.43°C) and plate dendrite (586.82~2615.24°C), are relatively higher than that from initial stage of solidification of spherical (409.95~1714.40°C) and cylindrical dendrite (515.13~1798.46°C).

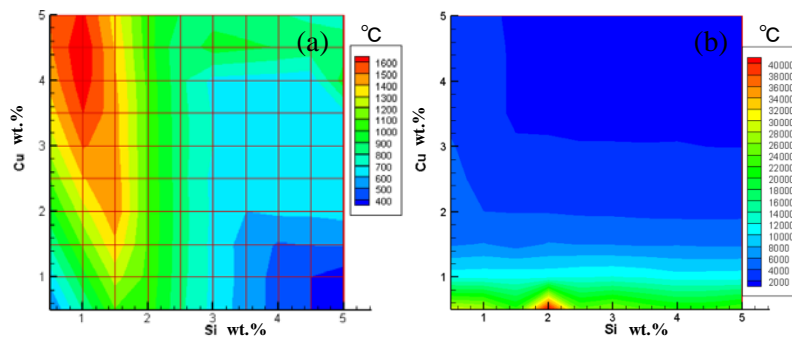


**Figure 4.** Al-Cu-Si hot crack susceptibility maps of the two limit cases: (a) Lever-rule; (b) Scheil model

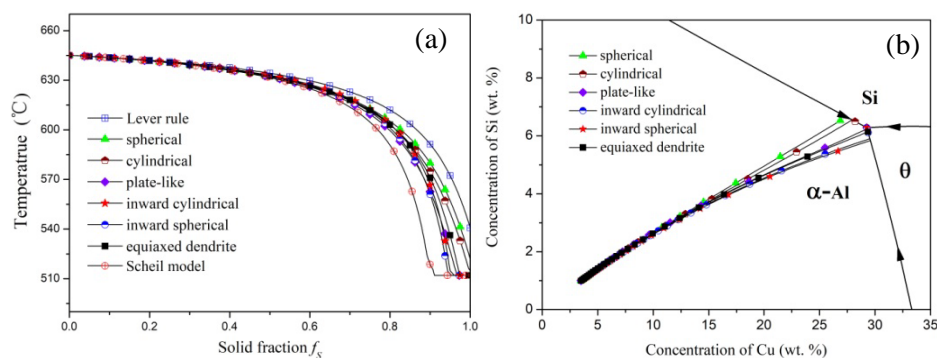


**Figure 5.** Calculated results of Al-1.0Si-3.5Cu with different assumptions of dendrite morphologies: (a)  $T-f_s$  curves; (b) solidification paths

## 5. Acknowledgments

This work was financially supported by the National Natural Science Foundation of China (Grant Nos. 51604162), the Opening fund of Hubei Key Laboratory of Hydroelectric Machinery Design & Maintenance (2017KJX12). And we wish to thank institute of solidification processing of materials in Harbin Institute of Technology, for providing the thermodynamic data used in this study.

## 6. References

- [1] Eskin DG, Suyitno KL and Katergman L 2004 *Prog. Mater. Sci.* **49** 629
- [2] Sheikhi M, Malek G F and Assadi H 2015 *Acta Mater.* **82** 491
- [3] Clyne T W, Davies G J 1981 *Br. Foundrym.* **74** 65
- [4] Mohammed M H, Asbjorn M and Hallvard F 2006 *Metall. Mater. Trans. B* **37** 3069
- [5] Jiangwei L, Sindo K 2017 *Acta Mater.* **125** 513
- [6] Coniglio N, Cross C E 2009 *Metall. Mater. Trans. A* **40** 2718
- [7] Rappaz M, Drezet J M and Remaud M 1999 *Metall. Mater. Trans. A* **30** 449
- [8] Sindo K 2015 *Acta Mater.* **88** 366
- [9] Jiangwei L, Sindo K 2015 *Acta Mater.* **100** 359
- [10] Guangwei Z, XinZhong L, Daming X et al 2012 *China Foundry.* **3** 269
- [11] Guangwei Z, Chong D, Xicong Y et al 2018 *J Phase Equilib. Diff.* **39** 212
- [12] Guangwei Z, Chong D, Xinsheng G et al 2017. *China Foundry.* **14** 443
- [13] Guangwei Z, Chong D, MingChun G 2019 *Int J Cast Metal Res.* **32** 36
- [14] D.M. Xu 2001 *Metall. Mater. Trans. B,* **32** 1129